Available online at www.pelagiaresearchlibrary.com

Pelagia Research Library

Advances in Applied Science Research, 2010, 1 (1): 34-43

Narrow Range of Y^{+++}-Dopings on $LiMn_{2-x}Y_xO_4$ for Promoting Structural, Microstructural and Cathodic Capacity Features of LiMnO-Spinel

M. M. Abou-Sekkina[b], Khaled M. Elsabawy[*a, b] and F. G. Elmetwaly[b]

[a]*Materials Science Unit, Faculty of Science, Taif University, Alhawyah-888-Saudi Arabia*
[b]*Materials Science Unit-Chemistry Department-Faculty of Science-31725-Tanta University-Egypt*

ABSTRACT

Samples with general formula $LiMn_{2-x}Y_xO_4$ (where x= 0.025,0.05 mole) were successfully synthesized through thermal decomposition of $LiMnC_2O_4$ (OAc) precursor, whereas $LiMnC_2O_4$ (OAc) precursor was synthesized by the room temperature solid state reaction.The structural , micro-structural and electrochemical features of pure spinel and yttrium doped samples were investigated .XRD-analysis indicated that all of the prepared samples are mainly belong to cubic crystal form with Fd3m space group .Only Y_2O_3 begins to appear as secondary impurity phase with maximum doping ratio x = 0.05 mole in minor . The electrochemical investigations included cyclic voltammetry, charge–discharge cycling of coin model cells were performed and indicated that substituted spinel with x = 0.025 mole ($LiMn_{1.975}Y_{0.025}O_4$) exhibits experimental discharge capacity equal to 128 $mAhg^{-1}$ which is better than that recorded for undoped spinel $LiMn_2O_4$ (126 $mAhg^{-1}$) .A visualization studies were also incorporated to prove crystal structure of Y-doped-spinel.

Keywords: Li-ion Battaries; Doped-Spinel; Crystal Structure; SEM; XRD.

INTRODUCTION

The lithium ion batteries are widely available for portable consumer applications such as lap top computers and cellular telephones. These batteries, consisting of lithium intercalation compounds as positive electrode, graphite or carbon as negative electrode, and an organic electrolyte are under consideration for the electric vehicle and the hybrid electric vehicle applications. The technological challenges confronting their scale up and commercialization are the capacity fade characteristics and the thermal safety. The cathode materials such as $LiCoO_2$ [1-2], $LiNiO_2$ [3-4], $LiNi_yCo_{1-y}O_2$ [5-6] are currently used in the lithium-ion batteries. Although the commercially available lithium-ion cells for portable applications use $LiCoO_2$ and $LiCo_yNi_{1-y}O$, they are considered to be more expensive and toxic than that having a $LiMn_2O_4$ cathode. The $LiMn_2O_4$ has been studied extensively as a cathode material for Li-ion batteries because it is relatively inexpensive and has environmental advantages,

compared with $LiCoO_2$, $LiNiO_2$, and $LiNi_yCo_{1-y}O_2$ [1, 2, 3, 4, 5 and 6]. However, $LiMn_2O_4$ shows problems related to poor cycling behavior because of a fast capacity fading in the three voltage range due to the phase transformation from cubic structure to tetragonal structure and also in the four voltage range mainly due to the Mn (Mn^{3+}) dissolution during lithium ion intercalation/deintercalation [7]. Reducing the amount of the Mn^{3+} ion in structure may help in improving the cycling performance of Mn spinel [8-10]. Transitional metals in the same row in the periodic table may be considered as the possible candidates for the substitution because of their similar ionic radii. The use of metal ions with similar radii will not cause a dramatic structural change as a result of the substitution [11-15]. In an effort to better understand the performance issues of the Mn spinels, research was undertaken to prepare the manganese-substituted spinels by partially substituting Mn separately with Co, Ni, Fe and Cr studying their structures, electrochemical behavior, diffusion phenomena and thermal characteristics. A sol–gel process was used for the synthesis in order to achieve the homogeneity and narrow particle size distribution of the final product [16-19]. The electrochemical and thermal properties of the substituted $LiMn_2O_4$ spinels were compared with those of $LiMn_2O_4$.

The major goal of the present article is to investigate narrow range of yttrium (III) ions doping on manganese sites ($0.025 \leq x \leq 0.05$) To promote:

1-Structural and micro-structural features of cubic spinel (Li-Mn-O).
2- Cathodic features (specially charge/discharge specific capacity and cycleability).

MATERIALS AND METHODS

I. Synthesis of Li-Mn-O spinels:

Li-Mn-O pure and Y-substituted spinels were prepared by thermal decomposition of $LiMnC_2O_4$ (AC) precursor which mixed with accurate molar ratios of yttrium oxide whereas $LiMnC_2O_4$ (AC) precursor was synthesized by the room temperature solid state reaction. In this method, LiOH and oxalic acid were mixed in a molar ratio of 1:1 and ground in a gate mortar until the mixture becomes sticky. Then, manganese acetate (in solid state) was added to the sticky mixture with the same molar amount, and ground for 30 min. In this process, the vinegar odor could be smelt. The obtained materials were further dried at 80-100^oC to remove water and acetic acid adsorbed on the product, and finally $LiMnC_2O_4$ (AC) precursor was obtained, then the $LiMnC_2O_4$ (AC) precursor was pressed into tablets, the lithium manganese oxides was prepared by sintering tablets of $LiMnC_2O_4$ (AC) precursor in air at 780^oC for 50 hrs with a heating rate of 10^oC / min without intermediate regrinding or other heating treatments, after sintering and cooling with a possible lowest rate (5 ^oC/min.) .

The formation and thermal decomposition of $LiMnC_2O_4$ (AC) precursor take place by grinding LiOH and Oxalic acid,

$$LiOH + H_2C_2O_4 \longrightarrow LiHC_2O_4 + H_2O \quad \text{.....(1)}$$

This, $LiHC_2O_4$ further reacts by grinding with manganese acetate as follow ;

$$LiHC_2O_4 + Mn(AC)_2\ 4H_2O \longrightarrow LiMnC_2O_4\ (AC) + HAC + 4H_2O \quad \text{.....(2)}$$

The strong vinegar odor was smelt because of the formation of acetic acid during grinding. According to the composition and synthesis principles, the structure formula of the precursor could be expressed as;

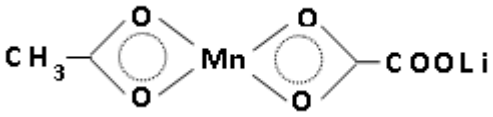

In which Mn^{2+} was coordinated, respectively with the oxygen atoms of CH_3COO^- and LiOOC-COO. Accordingly, the Li and Mn^{2+} were amalgamated in one precursor molecule.

II.Structural characterization:

II.A. X-Ray diffraction (XRD):

The X-ray diffraction measurements (XRD) were carried out at room temperature on the fine ground pure and Y-substituted spinels in the range (2θ =10-90^o) using Cu-Kα radiation source and a computerized [Steo-Germany] X-ray diffracto-meter with two theta scan technique. A visualized studies of crystal structure were made by using Diamond Molecular Structure version 3.2 package, Germany .

II.B. Scanning Electron – Microscope:

Scanning electron microscope (SEM) measurements were carried out using small pieces of prepared samples on different sectors to be the actual molar ratios by using "TXA-840,JEOL-Japan" attached to XL30 apparatus with EDX unit, accelerant voltage 30kv, magnification 10x up to 500.000x and resolution 3. nm. The samples were coated with gold.

III. Electrochemical measurements:

The coin cells model (2016 size) were used for electrochemical. The coin cells comprised of $LiMn_{2-x}Y_xO_4$ as a cathode, lithium foil anode, and an electrolyte having 0.5 M $LiPF_6$ in a 1:1 wt.% of ethylene carbonate and diethyl carbonate (EC/DEC, EM Industry, Inc. H_2O<30 ppm). A Celgard 2400 micro-porous polypropylene separator was used in these cells. The cell preparation was carried out in the Argon-filled dry box.The cyclic voltammetry curves were obtained at room temperature using the above coin cells at a scan rate of 0.02 mV s^{-1}. Another group of fresh coins cells were also cycled glavanostatically using an Arbin cycler in the potential range of 2.5–4.5 V for $LiMn_{2-x}Y_xO_4$ (Y = 0.025 and 0.05 mole).

The cells were first cycled three times and then, charged to 4.4 V. The cells were charged using a constant voltage charging procedure for 40 h. The cut-off voltage for charging was 4.4 V. The charged coin cells were opened in an agron-filled glove box and the cathode material was recovered from the cells.

RESULTS AND DISCUSSION

I. Phase Identification:

Fig.1$_{a-c}$ shows the X-ray diffraction patterns of pure spinel and Y-doped spinels with formula $LiMn_{2-x}Y_xO_4$ (where x= 0.025,0.05 mole) powders. Analysis of the corresponding 2θ values and the interplanar spacings d (A^o) proved that the compounds are mainly belongto a single-phase spinel structure. with Fd3m space group in which the lithium ions occupy the tetrahedral (9a) sites as clear in Fig.1$_d$. The Mn^{3+} and Mn^{4+} ions as well as the doping metal ions, as in $LiMn_2O_4$ structure, occupy the octahedral (16d) sites [19]. For simplicity, these

structures can be expressed as $[Li]^{tetrahedral}$ $[M_yMn_{2-y}]^{octahedral}[O_4]$ [20] as described in fig.1d and Table 1. Doping did not appear to change the basic $LiMn_2O_4$ structure, but slightly change the lattice parameters due to atom size effect.
As clear in Figs.1_{a-d} the Li-Mn-O spinel doped with Y^{3+} of at the expense of Mn^{3+} crystallized in octahedral units [MnO_6] without any kind of noticeable distortion as expected with Fd3m space group . Only yttrium oxide as secondary phase appears in minor trace in the back ground at x = 0.05 mole which confirm success of doping in the investigated range.

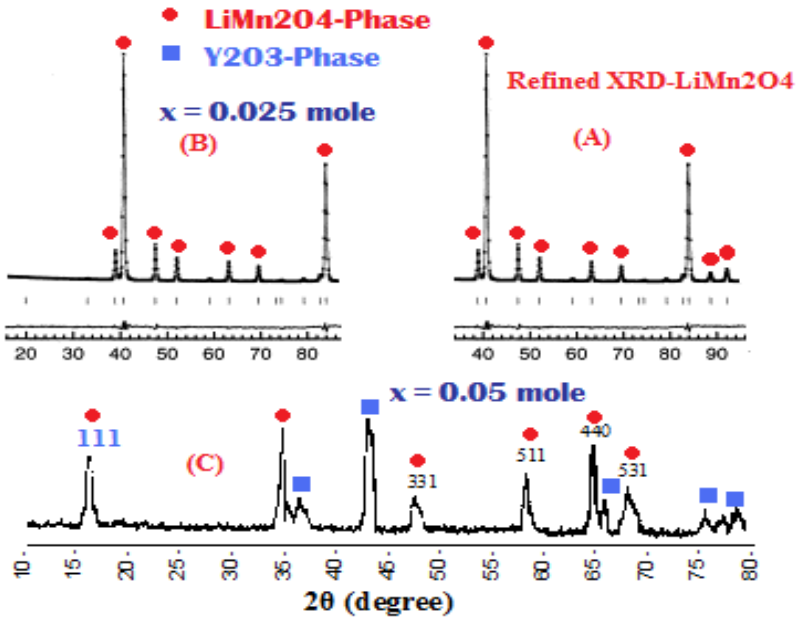

Fig.(1_{a-c}): X-ray diffraction patterns of $LiMn_{2-x}Y_xO_4$ spinel doped with Y^{3+}
(a): undoped $LiMn_2O_4$
(b): doped with x = 0.025 mole
(c): doped with x = 0.050 mole

It is well known that spinel $LiMn_2O_4$ as a cathodic material is too poor to be substituted or replaced by $LiCoO_2$ due to the gradual degradation of its capacity on cycling. The degradation mechanisms have been proposed as (a) structural damage due to Jahn-Teller distortion, (b) dissolution of the spinel into the electrolyte, (c) oxidation of the electrolyte on the surface of the cathode at the highly charged state [21-25].

Accurate retvield analysis of structure indicated that all samples have the finger print peaks of Li-Mn-O spinel (red circles in Fig 1_{a-c}) with high degree of crystallinity. The lattice constants of cubic spinels were calculated and found to be a = 8.2879(1) A^o for x = 0.025 mole and a = 8.288(4) A^o for x = 0.05 mole which are bigger than undoped one (a = 8.269(3)) since the radii of the sixth coordinate Y^{3+} and Mn^{3+} are 0.090 and 0.066 nm, respectively. So that the unite crystal volume expands, that what was expected, but in opposite with Xu et al.[26] .

These results in full agreement with those reported by Wolska et al.[27] who stated that substitution with very small quantities of Fe^{+++} ions first restrains the partial ordering of Mn^{3+} and Mn^{4+} ions in the spinel super-lattice and then stabilizes cubic spinel structure of $LiMn_2O_4$.

Confirmation of synthesized pure spinel and Y-doped spinels with formula $LiMn_{2-x}Y_xO_4$ (where x= 0.025,0.05 mole) structures were performed through theoretical treatment by visualizing of structures of both experimental and theoretical lattice coordinates of spinel structure (Fig.1_d) via Diamond Impact Crystal package.

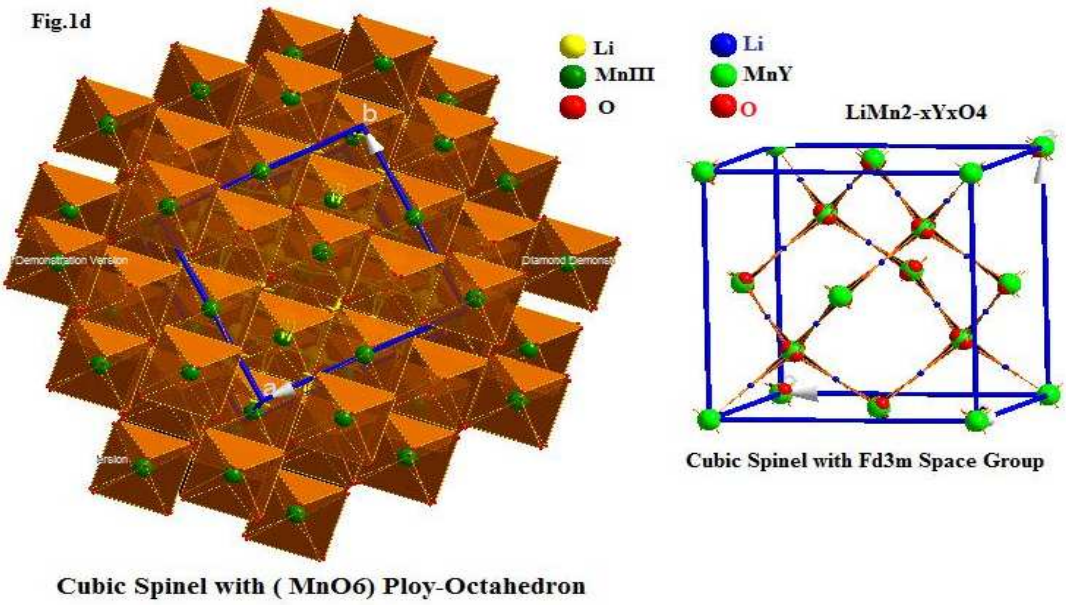

The study made was concerned by matching and comparison of calculated and theoretical data as bond distances , oxidation states and bond torsion on the crystal structure formed. The study and comparison between experimental and theoretical data exhibited good fitting of peak positions between experimental and theoretical data confirming that Y-III substitutes successfully on crystal structure on Mn(III) sites in the investigation range .

The analysis of bond distances recorded in Table .1 one can notify that there are no violation on the MnY-O bond distances observed which reflect the narrow ratio of dopant element (Y^{+++}) ion does not cause any kind of distortion inside poly–octahedrons and consequently lattice structure of spinel.

Furthermore the torsions on the bonds angle inside lattice and superlattice of Y-doped spinels does not destroy spinel structure which reflect suitability and fitting between doping element and substituted managanese (III) sites.

Table .1: Some Selected lattice coordinates,bond distances inside unit cell of Y-substituted Spinel Li-Mn-O

Table 1		Lattice Coordinates			Bond Distance
Atom 1	**Atom 2**	**x/a**	**y/b**	**z/y**	**d A°**
Li1	O1	0.0124	0.0124	-0.0124	1.7415
Li1	O1	0.0124	-0.0124	0.0124	1.7415
Li1	O1	-0.0124	0.0124	0.0124	1.7415
Li1	O1	0.2624	0.2376	0.2376	1.7415
Li1	O1	0.2376	0.2376	0.2624	1.7415
Li1	O1	0.2376	0.2624	0.2376	1.7415
Li1	Mn1|Y1	0	0	0	1.7927
Li1	Mn1|Y1	0.2500	0.2500	0.2500	1.7927

Li1	O1	-0.0124	-0.0124	-0.0124	1.9705
Li1	O1	0.2624	0.2624	0.2624	1.9705
Mn1|Y1	O1	0.4876	-0.0124	0.4876	0.1778
Mn1|Y1	O1	0.4876	0.0124	0.5124	0.1778
Mn1|Y1	O1	0.5124	-0.0124	0.5124	0.1778
Mn1|Y1	O1	0.5124	0.0124	0.4876	0.1778
Mn1|Y1	Li1	0.3750	-0.125	0.6250	1.7927
Mn1|Y1	Li1	0.6250	-0.125	0.3750	1.7927
Mn1|Y1	Li1	0.6250	0.1250	0.6250	1.7927
Mn1|Y1	Li1	0.3750	0.1250	0.3750	1.7927
O1	Mn1|Y1	0.2500	0.2500	0.2500	0.1778
O1	O1	0.2376	0.2376	0.2624	0.2904
O1	O1	0.2624	0.2376	0.2376	0.2904
O1	O1	0.2376	0.2624	0.2376	0.2904
O1	Li1	0.3750	0.1250	0.3750	1.7415
O1	Li1	0.3750	0.3750	0.1250	1.7415
O1	Li1	0.1250	0.3750	0.3750	1.7415
O1	Li1	0.1250	0.1250	0.1250	1.9705

II. Scanning Electron Microscopy:

The morphology of powdered samples for undoped and doped sample fired at 750^{o}C in air for 50 hr, were investigated by scanning electron microscope (SEM) after coating with gold. Fig.(2_{a-c}) represents the captured images for undoped $LiMnO_4$ powder and Y-doped spinels. with low – magnification of 750 times, the morphology of this powder reveals that the powder exhibits irregular porous agglomerates.

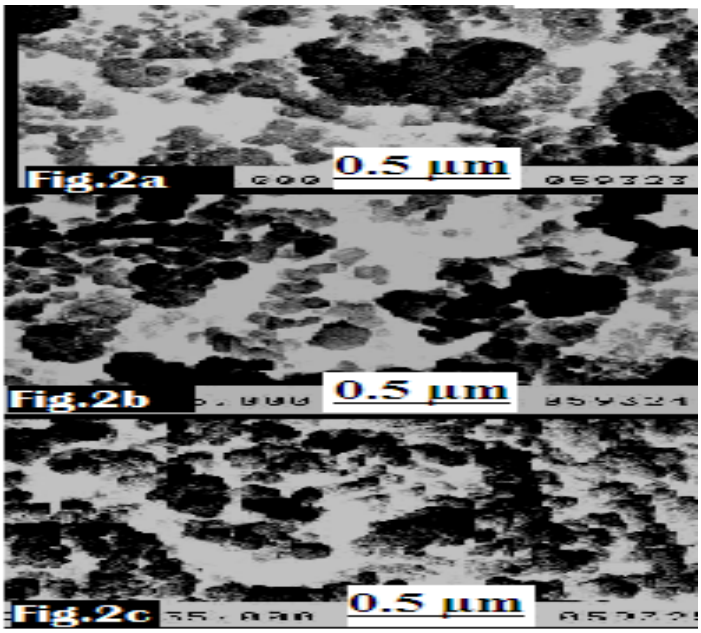

Fig.2. SE-micrographs captured for pure and Y-substituted spinels
(Amplification factor = 0.5 µm)
(a): undoped $LiMn_2O_4$
(b): doped with x = 0.025 mole
(c): doped with x = 0.050 mole

It can be more clearly observed that there are many micro – holes in the surface of the particles, this porous morphology is beneficial for the diffusion of electrolyte into the interior of the particle during fabrication of the battery. The formation of porous morphology is attributed to the escape of the gases such as CO_2 and H_2O from the interior of the particles during the heat treatment. In other words, the organic constituents in $LiMnC_2O_4$(AC) precursor has bubbling effect. The morphology of the same sample ($LiMn_2O_4$) doped with yttrium (x = 0.025 and x = 0.05 mole) with magnification of 35000 times. Fig.(b,c), reveal that the sample have regular nano – sized grains of average size 147 nm and the average particle size is ~ 15.6 nm.

These averages of grain and particle size of pure and Y-doped spinels are fully consistent with those reported by Lu et al.[28] who synthesized uniform spinel by using emulsion technique with spherical powders with a size distribution which ranged from 0.1-0.15 µm .

III. Electrochemical measurements:

III.A. Specific Capacities Investigations:

Fig. 3_{A-C} shows the initial charge–discharge curves of Li/ $LiMn_{2-x}Y_xO_4$ coin cells where x = 0, 0.025 and 0.05 mole respectively at a constant charge–discharge rate of C/20 over the voltage range of 4.5–3.5 V. The theoretical and experimental capacities are compared.

The theoretical capacity of the $Li/LiMn_2O_4$ cell is 148 mA h g^{-1} [29] on the basis that one Li per Mn_2O_4 unit is reversibly intercalated and deintercalated at 4.12 V. But, $LiMn_2O_4$ shows actual value of about 126 mA h g^{-1} corresponding to 0.82–0.90 of total Li in $LiMn_2O_4$ reversibly utilized within the voltage range of 3.5–4.5 V. While the specific capacities recorded for yttrium-substituted spinels were 128 and 91 mA h g^{-1} respectively .

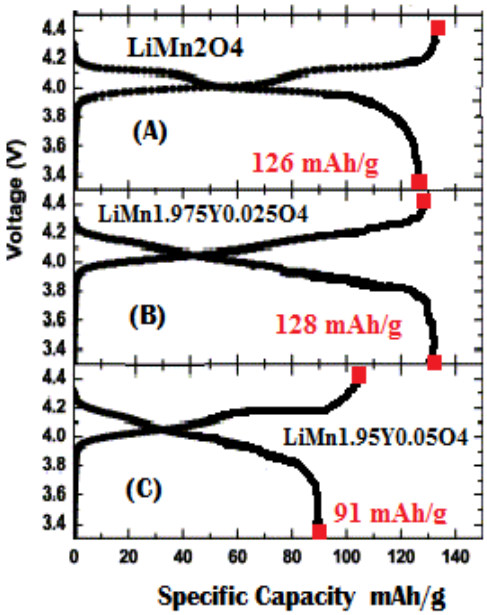

Fig. 3a-c. First cycle charge and discharge curves of type 2016 coin cells at C/20 rate
Cell—Li–0.5 M $LiPF_6$ in (1:1 wt.% EC+DEC)–$LiMn_{2-x}Y_xO_4$
(where x =0.025, and x = 0.05 mole respectively)

It was observed that for the first ten cycles the capacity retentions (loss with recycleability) were promoted as yttrium doping increases recording maximum for x = 0.025 mole (0.31 % loss per cycle) and 0.93 % loss per cycle for $LiMn_{1.95}Y_{0.05}O_4$ and minimum one for the undoped parent $LiMn_2O_4$.

Accordingly the enhancement of specific capacity (see Fig.4) and recycleability of yttrium-doped samples specially that with optimal doping content x = 0.025 mole is due to Y(III) resists redox reactions on its immersed electrolyte and stabilize spinel crystal structure by reinforcing lattice stability towards Jahn-Teller distortion inside $MnYO_6$ –poly-octahedrons.

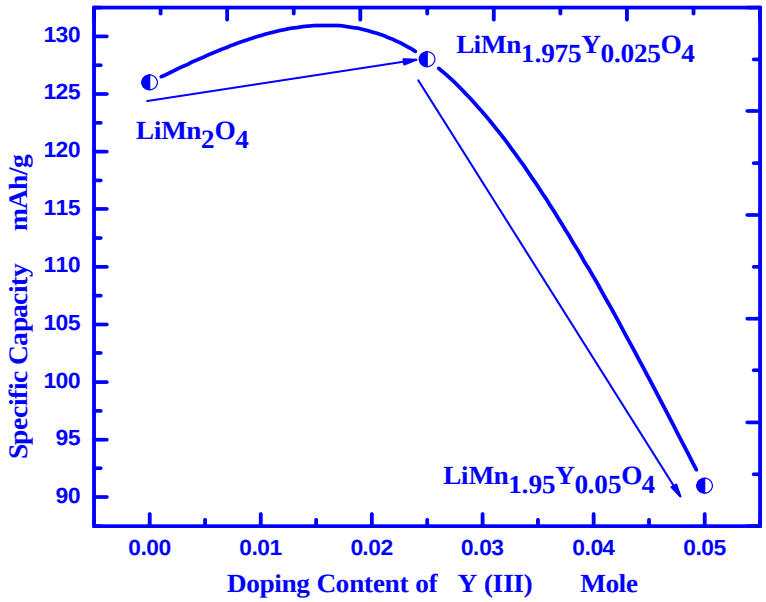

Fig.4: Specific Charging Capacity versus Y-III-Doping Content

III.B. Cyclic Voltammetry Measurements:

The potential scan for cyclic voltammetry for $LiMn_{2-x}Y_xO_4$ where x = 0 ,0.025 and 0.05 mole samples was conducted within a potential range from 3.5 to 4.5 V versus Li/Li^+. The cyclic voltammetry curves as shown in Fig.5a-c have some important observations:

There are two anodic and cathodic peaks for pure spinel and Y-substituted spinels .The peak potentials of the substituted spinels in the anodic region slightly shifted to high potential and those in the cathodic region also shifted towards high potential with respect to the $LiMn_2O_4$.

The peak current densities as well as the area under the current–voltage curve for the substituted spinels lower and smaller than those of $LiMn_2O_4$ by very small ratios.

The two pairs of the oxidation and reduction peaks of $LiMn_2O_4$ spinel were located around 4.21 and 4.06 V, corresponding to the two-stage reversible intercalation/deintercalation processes of lithium. The results obtained in this study are consistent with those reported previously [18 and 30]. The oxidation of Mn^{3+} to Mn^{4+} contributes to the oxidation peaks in the investigated voltage range for the $LiMn_2O_4$ and so it is reasonable to assume that only Mn^{3+} in both substituted spinels causes the oxidation and reduction peaks [20] and that the

amount of Mn^{3+} is decreased by doping, thereby resulting in a decrease in the observed peak current.

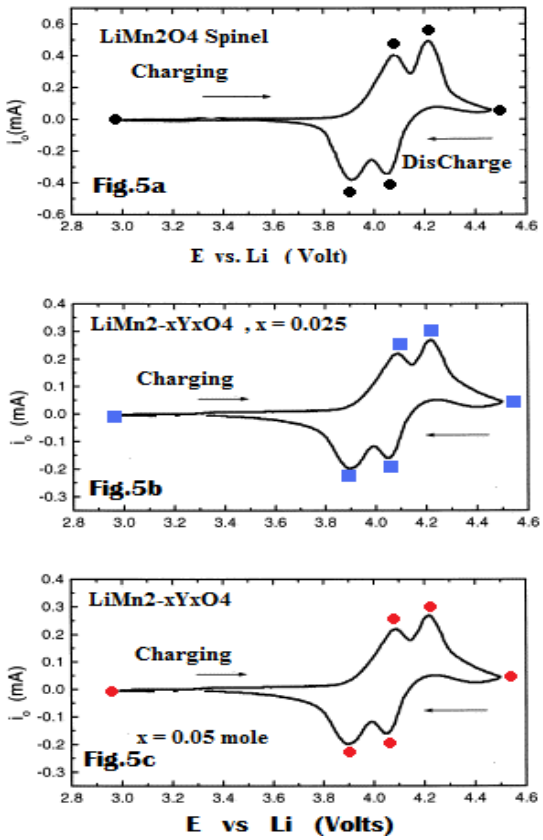

Fig. 5$_{a-c}$. Cyclic voltammetry curves of $LiMn_2O_4$ and substituted $LiY_xMn_{2-x}O_4$ (x =0.025 and 0.05 mole) spinels in 0.5 M $LiPF_6$ in 1:1 wt.% EC+DEC electrolyte Scan RATE=0.02 mV s^{-1}
(a): undoped $LiMn_2O_4$
(b): doped with x = 0.025 mole
(c): doped with x = 0.050 mole

CONCLUSION

The conclusive remarks can be briefed as follow :

1- capacity retentions (loss with recycleability) were promoted as yttrium doping increases recording maximum for x = 0.025 mole (0.31 % loss per cycle) and 0.93 % loss per cycle for $LiMn_{1.95}Y_{0.05}O_4$ and minimum one for the undoped parent $LiMn_2O_4$.

2- charging cathodic capacity enhanced by Y-dopings and recorded 128 and 91 mA h g^{-1} respectively for yttrium-substituted spinels with x= 0.025 and 0.05 mole respectively .

Accordingly the enhancement of specific capacity and recycleability of yttrium-doped samples specially that with optimal doping content x = 0.025 mole is due to Y(III) resists redox reactions on its immersed electrolyte and stabilize spinel crystal structure by reinforcing lattice stability towards Jahn-Teller distortion inside $MnYO_6$ –poly-octahedrons .

REFERENCES

[1] T. Nagaura and K. Tazawa *Prog. Batteries Solar Cells* 9, **1990**, 20.

[2] K. Ozawa *Solid State Ionics* 69, **1994**, 212.
[3] W. Ebner, D. Fouchard and L. Xie *Solid State Ionics* 69, **1994**, 238.
[4] J.R. Dahn, U. Von Sacken, M.R. Jukow and H. Al-Janaby *J. Electrochem. Soc.* 138, **1991**, 2207.
[5] C. Delmas, I. Saadoune and A. Rougier *J. Power Sources* 43–44, **1993**, 595.
[6] R.J. Gummow and M.M. Thackeray *J. Electrochem. Soc.* 140, **1993**, 3365.
[7] J.M. Tarascon, W.R. Mckinnon, F. Coowar, T.N. Boowner, G. Amatucci and D. Guyomard *J. Electrochem. Soc.* 141, **1994**, 1421.
[8] D. Guyomard and J.M. Tarascon *Solid State Ionics* 69, **1997**, 22.
[9] X. Qiu, X. Sun, W. Shen and N. Chen *Solid State Ionics* 93, **1997**, 335.
[10] Y.-K. Sun *Solid State Ionics* 100, **1997**, 115.
[11] J.M. Tarascon, E. Wang, F.K. Shokoohi, W.R. Mckinnon and S. Colson *J. Electrochem. Soc.* 138, **1991**, 2589.
[12] T. Ohzuku, M. Kitagawa and T. Hirai *J. Electrochem. Soc.* 137, **1990**, 769.
[13] R. Bittihin, R. Herr and D. Hoge *J. Power Sources* 43-44, **1993**, 223.
[14] Y. Toyoguchi, *Eur. Pat. Appl*. 0390, **1990,** 185.
[15] S. Bach, M. Henry, N. Buffer and J. Livage *J. Solid State Chem.* 88, **1990**, 325.
[16] T. Tsumura, A. Shimizu and M. Inagaki *J. Mater. Chem.* 3, **1993**, 995.
[17] P. Barboux, J.M. Tarascon and F.K. Shokoohi *J. Solid State Chem.* 94, **1991**, 185.
[18] W. Liu, G. Farrington, F. Chaput and B. Dunn *J. Electrochem. Soc.* 143, **1996**, 879.
[19] G. X. Wang, H. K. Liu and S. X. Dou ,*Solid State Ionics*,,120, 1-4, **1999** , 95-101
[20] L. Guohua, T. Uchida and M. Wakihara *J. Electrochem. Soc.* 143, **1996**, 178.
[21] A.R. West In: *Basic Solid State Chemistry*, Wiely, New York , **1991**, 57.
[22] R. Koksbang, J. Barker, H. Shi and M.Y. Sa. *Solid State Ionics* 84, **1996**, 1–21.
[23] M.M. Thackeray, W.I.F. David and J.B. Goodenough. *Mater. Res. Bull.* 17, **1982**, 785.
[24] M.M. Thackeray. *J. Electrochem. Soc.* 142, **1995**, 2558–2563.
[25] R.J. Gummow, A. de kock and M.M. Thackeray. *Solid State Ionics* 69, **1994**, 59.
[26] C.Xu,Y. Tain,Y.C.Zhai,L.Y.Liu,*Materials Chemistry and Physics* 98, **2006,** 532-538.
[27] E.Wolska ,M.Tovar ,B.Andrzejewski ,W.Nowicki ,P.Pisora ,M.Knapp, *Solid State Science* 8, **2006**, 31-36.
[28] C.H.Lu and S.W.Lin ,*Journal of Power Sources* ,93, **2001,** 14-19.
[29] H. J.Bang, V. S. Donepudi and J.Prakash, *Electrochimica Acta*, 48, 4, **2002**, 443-451
[30] J.M. Tarascon and D. Guyomard *J. Electrochem. Soc.* 138, **1991**, 2864.